

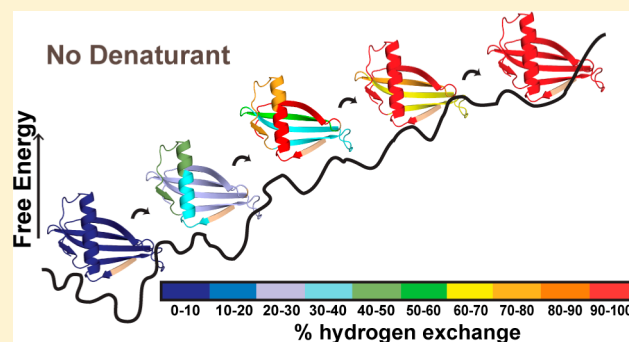
Secondary Structural Change Can Occur Diffusely and Not Modularly during Protein Folding and Unfolding Reactions

Pooja Malhotra and Jayant B. Udgaonkar*

National Centre for Biological Sciences, Tata Institute of Fundamental Research, Bengaluru 560065, India

S Supporting Information

ABSTRACT: A major goal of protein folding studies is to understand the structural basis of the coupling between stabilizing interactions, which leads to cooperative conformational change. The goal is challenging because of the difficulty in simultaneously measuring global cooperativity by determining population distributions of the conformations present, and the structures of these conformations. Here, hydrogen exchange (HX) into the small protein monellin was carried out under conditions where structure-opening is rate limiting for most backbone amide sites. Detection by mass spectrometry allowed characterization of not only segment-specific structure-opening rates but also the cooperativity of unfolding of the different secondary structural segments of the protein. The segment-specific pattern of HX reveals that the backbone hydrogen-bonding network disassembles in a structurally diffuse, asynchronous manner. A comparison of the site-specific transient opening rates of secondary and tertiary structure in the protein provides a structural rationale for the observation that unfolding is hierarchical and describable by exponential kinetics, despite being diffuse. Since unfolding was studied in native conditions, the sequence of events during folding in the same conditions will be the reverse of the sequence of events observed during unfolding. Hence, the formation of secondary structural units during folding would also occur in a non-cooperative, diffuse, and asynchronous manner.



INTRODUCTION

The cooperativity of protein folding and unfolding reactions is determined by the structural coupling within a complex network of stabilizing interactions. If all the intramolecular interactions are strongly coupled to each other, then unfolding could conceivably be fully cooperative (or “two-state”), occurring in an all-or-none manner.^{1,2} If the coupling is very weak, then unfolding could conceivably be completely non-cooperative (or gradual), occurring through a continuum of states. If interactions within specific regions of the protein are coupled, but the interactions between these regions are not, then different parts of the protein would unfold independently, resulting in a modular disassembly of the protein molecule.^{3–8} It is, however, unclear how structural events in different parts of a protein are coupled in cooperative transitions, or why they are not coupled in gradual folding/unfolding transitions. To understand the structural rationale for a cooperative versus a non-cooperative protein folding transition has been a long-standing challenge.

Understanding the interplay between the individual structural events that occur during the folding of a protein, and the cooperativity of the overall process, remains an experimental challenge because of the difficulty in concurrently obtaining high-resolution structural information and monitoring the cooperativity of the process with the same probe. The best way to delineate the cooperativity of a folding reaction is to

monitor the populations of the different conformations present together and examine whether they interconvert in an all-or-none or gradual manner, with a change in either the folding conditions (in equilibrium studies) or the time of folding (in kinetic studies). One method that can directly differentiate between cooperative and non-cooperative unfolding transitions is hydrogen exchange (HX) coupled to mass spectrometry (MS): HX probes the backbone hydrogen-bonding network in the protein, providing high-resolution structural information,⁹ while MS monitors mass distributions, providing population distributions of the different conformations present.^{10–13}

In native conditions, HX into the small protein single chain monellin (MNEI) has been shown to be limited by the rates of transient opening (unfolding) of the structure at individual backbone amide sites.¹³ The HX-MS experiments revealed that unfolding occurred through a gradual, one-state transition in which all backbone amide sites opened in an uncorrelated manner.¹³ Despite being non-cooperative, the structure-opening transitions were found to proceed in well-resolved exponential kinetic phases, an observation usually associated with the formation of structurally distinct intermediate forms with modular structures. Upon the addition of low concen-

Received: December 8, 2015

Revised: April 1, 2016

Published: April 19, 2016

trations of denaturant, a subset of the backbone amide hydrogen sites did, however, open to HX in a correlated (cooperative) manner. MNEI is therefore an attractive system for studying how local structural changes occurring in different parts of the protein during folding/unfolding are coupled, and how this coupling establishes the cooperativity of the overall folding/unfolding reaction.

MNEI is a small, 97-residue sweet protein which folds and unfolds in multiple steps with several intermediates and parallel pathways present.^{14–21} Detailed structural characterization of the sequence of unfolding and refolding events and intermediate structures is, however, lacking. Native-state thiol labeling (SX)²² has provided information on how site-specific tertiary packing interactions are lost during unfolding, and has also revealed the presence of multiple barriers on the unfolding landscape. Nevertheless, since only four residues were probed by SX in that study, the continuous nature of the unfolding reaction, observed in the HX experiments,¹³ which probed the entire backbone hydrogen-bonding network in the protein, could not be observed. Correlation of the kinetics of the loss of specific packing interactions obtained from the SX data with the kinetics of the site-specific loss of main-chain structure from HX data should lead to a better understanding of the extent to which different intramolecular interactions are coupled during unfolding.

In the present study, the rates of transient opening of individual structural elements of MNEI have been determined by examining the fragments of the protein generated subsequent to exchange. HX into MNEI is expected to occur predominantly in the EX1 limit at pH 8, even under native conditions in the absence of denaturant, because the average intrinsic exchange rate constant calculated for MNEI is 150 s^{-1} at pH 8,²³ while 90% of the protein refolds at rates which are at least 100-fold slower.²² Indeed, the majority of the backbone amides were observed to exchange in the EX1 limit, in good agreement with previous work.¹³ Careful analysis of the exchange kinetics was used to identify the few backbone amide sites which exchange in the EXX or EX2 limit. A comparison of the segment-specific opening rates, obtained from the sites which undergo EX1 exchange, with those observed for the whole protein reveals that each kinetic phase of exchange, averaged across the whole protein, is associated with transient structure-opening events in all parts of the protein. The diffuse loss of structure under native conditions suggests a lack of any modular architecture in MNEI. A comparison of the HX data with previously obtained SX data further reveals that the kinetics of loss of local side-chain packing interactions, which precedes the dissolution of the proximal secondary structure in different parts of the protein, can explain the observation of discrete kinetic phases in a non-cooperative transition.

MATERIALS AND METHODS

Protein Purification. MNEI was purified as described previously.¹⁵ The purity (>95%) and mass ($11\,403 \pm 0.3 \text{ Da}$) of the protein were checked by electrospray ionization mass spectrometry (ESI-MS). The protein concentration was estimated using an extinction coefficient of $14\,600 \text{ M}^{-1} \text{ cm}^{-1}$ at 280 nm.¹⁵

Reagents. All experiments were carried out at 25 °C. The reagents used in the experiments were of the highest purity grade from Sigma. Guanidine hydrochloride (GdnHCl) of the highest purity grade was obtained from United States Biochemicals. The exchange buffer, used to initiate HX, was 20 mM Tris (H₂O) at pH 8, and 20 mM phosphate buffer at pH 7. The quench buffer, used to stop the exchange reaction,

was 100 mM glycine hydrochloride, containing 8 M GdnHCl, at pH 2.2 on ice. The pH values reported for the D₂O buffers were not corrected for any isotope effect.

Deuteration of MNEI. The protein was deuterated as described previously.¹³ Briefly, the lyophilized protein, dissolved in 10 mM Tris (D₂O), was incubated at pH 12.6 for 5 min. The pH was subsequently dropped to 1.6 and then slowly readjusted to 8 using DCl and NaOD, respectively. Exposure to pH 12.6 unfolded the protein and allowed deuteration at all exchangeable sites. The mass of the fully deuterated protein was checked by desalting the sample with ZipTip and injecting it directly into the mass spectrometer with a syringe pump.

Hydrogen Exchange Kinetics. The exchange reaction was initiated by a 15-fold dilution of 500 μM deuterated protein into exchange buffer. At different times of exchange at 25 °C, the reaction was quenched by adding 375 μL of quench buffer to 125 μL of the exchange reaction, on ice. The final quenched reaction, containing 6 M GdnHCl, was incubated for 1 min on ice to facilitate subsequent fragmentation. To ensure uniform processing of samples, this step was incorporated into experiments with the intact protein as well as with the fragments. For exchange in 1 M GdnHCl, the denaturant concentrations in the exchange and quench buffers were adjusted accordingly.

Sample Processing. The quenched samples were desalted using a Sephadex G-25 Hi-trap column from GE, on an ÄKTA basic HPLC system, and eluted into Milli-Q water, pH 2.6, on ice, in order to maintain quenched conditions.

Data Acquisition by ESI-MS. After desalting, the samples were injected into the HDX module (Waters Corp.) of the nanoACQUITY UPLC system coupled to a Synapt G2 HD mass spectrometer. A final desalting was achieved by loading the protein onto a C18 reverse phase trap column for 1 min at a flow rate of 100 $\mu\text{L}/\text{min}$, in 0.05% formic acid. The protein was eluted from the trap column in a 3 min chromatographic run, between 35 and 95% acetonitrile (0.1% formic acid). The temperature during chromatography was maintained at 4 °C in the Waters HDX cooling module to ensure minimal back exchange. The parameters used for ionization in ESI-MS were as follow: capillary voltage, 3 kV; source temperature, 80 °C; desolvation temperature, 200 °C. A cumulative ion count of $>10^6$ was obtained by combining 40 scans.

Electron-transfer dissociation (ETD) was the chemical fragmentation method used for generating fragments of MNEI subsequent to exchange.²⁴ The ETD reagent used for fragmentation of the intact protein was 1,4-dicyanobenzene. Radical anions of this reagent were generated using a glow discharge current of 35 μA . A total of 10^6 counts of the reagent per scan were obtained using a flow rate of 25 mL/min for the makeup gas (nitrogen). Optimum fragmentation was observed for the +11 charge state. The instrument parameters for fragmentation were as follow: sample cone voltage, 30 V; extraction cone voltage, 4 V; trap wave velocity, 300 m/s; wave height, 0.35 V; transfer collision energy, ramped from 10 to 14 eV.

In order to confirm the lack of hydrogen/deuterium migration (scrambling), the instrument parameters used in the present study were varied systematically to achieve harsher conditions more likely to cause scrambling. A previous study,²⁵ using the same mass spectrometer and ionization source as that used in the present study, had carried out an extensive investigation of the parameters that affect the extent of scrambling, and found that increasing the sample cone voltage had the maximum effect. Hence, the deuterium retention in MNEI, in 0 M GdnHCl, was measured at different sample cone voltages in the range of 10–60 V, keeping all other parameters fixed at the values mentioned above, which were shown to cause minimal scrambling. Migration of hydrogens/deuteriums prior to fragmentation should alter the number of deuteriums measured in a given fragment. As shown in Figure S1, the deuterium retention in each ETD ion did not vary significantly with cone voltage, at different exchange times, confirming the lack of scrambling under the present experimental conditions.

Pepsin Inhibition Assay. The inhibitory action of MNEI on pepsin activity was checked by digesting a known substrate of pepsin (SH3 domain of PI3K²⁶) in the presence of MNEI. First, 10 nM

pepsin was incubated with different concentrations of MNEI (1–50 nM) for 5 min at room temperature. Following this, 1 μ M SH3 was added. After 30 s of incubation, the solution was injected into the mass spectrometer at 4 °C, to quantify the amount of intact SH3 domain left.

The fluorescence intensity of a mixture of 20 μ M SH3 domain and 1 μ M MNEI was compared to the additive intensity of each protein measured separately, in order to determine if MNEI interacts with the SH3 domain. An excitation wavelength of 295 nm was used, and emission was collected at 360 nm.

Data Analysis. A. Analysis of ETD Fragments. The centroid spectra obtained from ETD fragmentation were analyzed using the BioLynx software to identify the individual c and z ions of the protein produced by chemical fragmentation. The intensity weighted isotopic abundances were used to estimate the average mass of each ion. The number of deuteriums retained in each ion was determined by comparing the mass of the given ion obtained from an exchanged protein sample with the mass of the ion obtained from the protonated protein. Consecutive c and z ions were used to monitor the extent of exchange in different sequence segments of the protein. For example, the average mass of the c39 ion (spanning residues 1–40) minus the average mass of the c4 ion (spanning residues 1–5) yielded the number of deuteriums retained at the backbone amide sites in the sequence segment spanning residues 6–40. Table S1 shows how the ETD ions obtained for MNEI were used to calculate the mass of each sequence segment of the protein. It should be noted here that even though multiple subtractions were used to arrive at the mass of a given sequence segment, none of the subtractions involved overlapping sequence segments. The mass of a smaller segment was subtracted from that of a larger one, only when it was completely contained within the larger segment.

B. Analysis of Gaussian Distributions. The combined spectra were background subtracted and smoothed in the MassLynx 4.1 software. The smoothed spectra of each ETD ion were fit to a Gaussian distribution function in Origin Pro 8 in order to determine the width (full width at half-maximum), height and centroid of each mass distribution as a function of time.

C. Analysis of Kinetic Traces. The number of deuteriums retained in a fragment ion was determined as a function of the time of exchange, to obtain the kinetic traces for HX into the corresponding sequence segment in the protein. The traces were fit to a single, double or a triple exponential equation to determine the rates and amplitudes of HX into each segment. The percentage of exchange at time t , in each segment, was calculated as

$$\frac{\Delta D_t}{\Delta D_{\text{total}}} \times 100 \quad (1)$$

where ΔD_t denotes the number of deuteriums that have undergone exchange at time t in a given sequence segment, and ΔD_{total} denotes the total number of deuteriums which could be monitored in the same segment. Hence, the extent of exchange into each segment increases from 0 to 100% as the protein structure opens. For each of the three kinetic phases of HX, the mean rate of HX (R) averaged over all the sequence segments is given by

$$R = \frac{\sum \alpha_i}{\sum \alpha_i \tau_i} \quad (2)$$

where α_i is the number of amide sites that undergo HX into sequence segment i and τ_i is the observed time constant of HX into sequence segment i for the same kinetic phase.

RESULTS

Fragments Obtained from ETD of the Intact Protein.

The native state of MNEI was found to be resistant to digestion by acid proteases such as pepsin, which are usually used to generate fragments of a protein in HX-MS experiments.^{27,28} Inhibition assays showed that MNEI is, in fact, an inhibitor of pepsin activity (Figure S2; see Methods and Discussion). The

intact protein, after HX, was therefore fragmented by ETD in the mass spectrometer,²⁵ in order to obtain the pattern of HX into the different secondary structural elements. ETD causes breakage at N–C α bonds, resulting in c ions (N terminal half) and z ions (C terminal half) (Figure S3). The low efficiency of ETD in fragmenting an intact protein²⁹ resulted in relatively long fragments. Nevertheless, the entire sequence of the protein could be covered (Figure 1A). The mass of a sequence segment

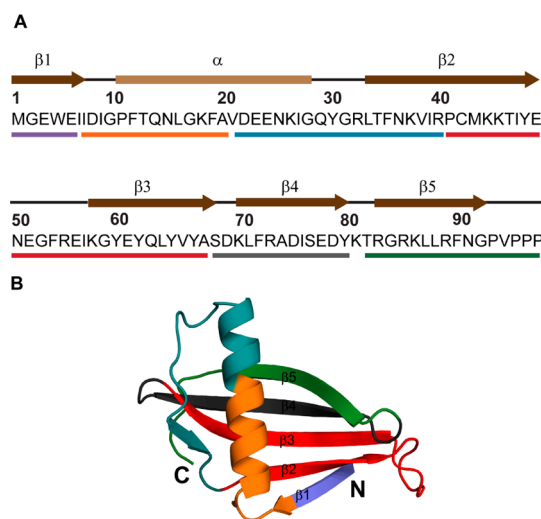


Figure 1. Fragmentation of MNEI. (A) The sequence of MNEI along with the secondary structural elements, denoted by dark brown arrows for the 5 β strands and a light brown bar for the sole α helix, are shown. The solid colored lines below the sequence indicate the sequence segments probed by HX-MS, by analyzing the ETD fragment ions as described in the Methods section. (B) The structure of MNEI (PDB ID: 1IV7) is shown with the different sequence segments colored according to panel A. The N and C termini of the protein have also been marked. The protein structure was drawn using the program PyMOL.

(Figure 1A) was measured by taking the difference in the average masses of continuous c or z ions, as described in the Methods and Table S1. These segments have been mapped onto the protein structure in Figure 1B. The lack of intramolecular hydrogen migration (scrambling), which is a major concern in any chemical fragmentation method,^{25,30} was confirmed, as described in the Methods.

In the presence of 1 M GdnHCl, cooperative exchange from two fragments of the protein led to bimodal mass distributions (see below), which yield two centroid masses for the same c or z ion. Since it was not possible to subtract the mass obtained from a unimodal distribution from that obtained from a bimodal spectrum, opening rates in 1 M GdnHCl could be obtained for only five of the seven segments probed in the absence of denaturant.

Segment Specific HX-MS Kinetics in 0 M GdnHCl. The mass distributions of all the c and z ions, produced by ETD, subsequent to exchange in the absence of denaturant, were found to shift in a unimodal manner at all times of exchange (Figures S4 and S5). Hence, the rates of transient opening to HX were measured by quantifying the shift in the centroid values of the individual fragments. The kinetic data obtained from analyzing the ETD fragment ions, are shown in Figure 2. The 44 ± 1 deuteriums retained in the protein at the earliest time after which exchange was quenched (5 s) served as

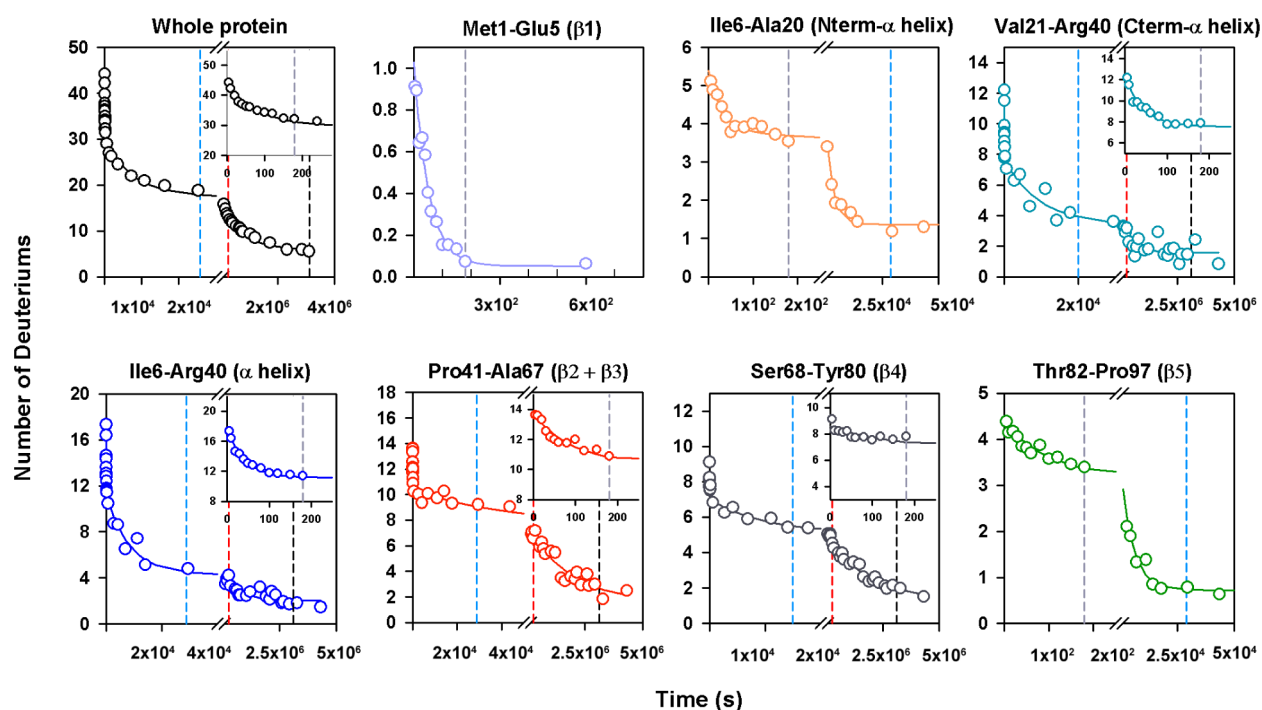


Figure 2. HX kinetics of different sequence segments of MNEI in 0 M GdnHCl, pH 8. The overall kinetics of HX into the whole protein is shown in the first panel.¹³ The deuterium retention of each sequence segment was obtained with respect to time of HX, in the absence of denaturant, from the ETD experiment, as described in the [Methods](#) section. The solid lines through the data represent fits to a single, double or triple exponential equation. The rate constants and amplitudes obtained from these fits are reported in [Table 1](#). The insets show the first 250 s of data for those segments which show a change in deuterium retention over that time scale. The dashed vertical lines represent different times of exchange: 3 min (gray), 8 h (blue), 72 h (red), and 36 days (black).

Table 1. HX Rates and Amplitudes of Different Sequence Segments of MNEI in 0 M GdnHCl, pH 8

Sequence segment	Fast phase		Slow phase		Very slow phase	
	Rate ($\times 10^{-2} \text{ s}^{-1}$)	Amplitude ^a	Rate ($\times 10^{-4} \text{ s}^{-1}$)	Amplitude ^a	Rate ($\times 10^{-6} \text{ s}^{-1}$)	Amplitude ^a
Whole protein^b	1 ± 0.5	13 ± 1 (33%)	1.4 ± 0.5	12 ± 1 (31%)	1.4 ± 0.007	14 ± 1 (36%)
Met1-Glu5 (β1)	2.2 ± 0.14	1 (100%)	-	-	-	-
Ile6-Ala20 (Nterm-α helix)	1.9 ± 1.2	2 (40%)	2.25 ± 0.8	3 (60%)	-	-
Val21-Arg40 (Cterm-α helix)	2.4 ± 0.2	5 (50%)	1.4 ± 0.4	3 (30%)	3.5 ± 1.9	2 (20%)
Ile6-Arg40 (α helix)	2.3 ± 0.4	7 (41%)	1.3 ± 0.1	7 (41%)	1.45 ± 0.07	3 (18%)
Pro41-Ala67 (β2+β3)	1.3 ± 0.35	3 (25%)	0.35 ± 0.23	3 (25%)	0.65 ± 0.16	6 (50%)
Ser68-Tyr80 (β4)	0.7 ± 0.01	2 (25%)	0.98 ± 0.18	2 (25%)	0.58 ± 0.14	4 (50%)
Thr82-Pro97 (β5)	1.3 ± 0.5	1 (25%)	2 ± 0.2	3 (75%)	-	-
Mean Rate (R)^c	1.5		0.9		0.7	

^aValues in italics correspond to the number of deuteriums which exchange; percentage of exchange is reported in brackets. ^bValues taken from ref 13. ^cCalculated using eq 2 described in [Methods](#). ^dThe shaded cells correspond to the two segments of the helix which together constitute the Ile6-Arg40 segment.

structural probes. The loss of information due to back exchange is negligible in the case of ETD, which occurs within the mass

spectrometer; consequently, the same number of deuteriums is monitored for the fragments as for the intact protein.¹³ A

comparison of the deuterium retention at the 5 s time point of exchange and the back exchange sample (which was prepared by directly quenching a fully deuterated sample, in order to determine the number of deuteriums lost during sample processing) revealed that around 28 deuteriums were lost within 5 s of exchange. These backbone amide deuteriums are likely to have undergone rapid exchange via local fluctuations, and therefore would not be reporting on structure-opening events in the protein.

In a previous study,¹³ it had been shown that overall HX into MNEI occurs in three kinetic phases: 13 ± 1 deuteriums exchange in the fast phase, 12 ± 1 in the slow phase and 14 ± 1 in the very slow phase. These kinetic phases were attributed to the formation of two intermediates, I_1 and I_2 , and the unfolded state, U, respectively. The exchange rates for most of the sequence segments monitored in this study compared well with the three rates of overall HX into the whole protein, and showed a wide dispersion over 5 orders of magnitude (Table 1). The mean rate calculated for each kinetic phase (see Methods), from HX into individual segments, was comparable to the rate observed for that phase for the whole protein. Also, for each kinetic phase the total number of deuteriums which exchanged out from all the segments was found to be similar to the number observed for the whole protein.

The kinetic data revealed that $\beta 1$ exchanged out in the fast kinetic phase, followed by $\beta 5$ which completed exchange in the fast and slow kinetic phases. $\beta 2$, $\beta 3$, $\beta 4$, and the helical segment (Ile6-Arg40) exchanged out significant fractions of their backbone deuteriums in all the three kinetic phases. While the N-terminal half (Ile6-Ala20) of the helix exchanged out in the fast and slow kinetic phases, the C-terminal half (Val21-Arg40) of the helix opened out in all three phases observed for the full helical fragment. Thus, the C-terminal half of the helix retained protection for much longer than the N-terminal half. In order to interpret the exchange kinetics shown in Figure 2, in terms of the structural transitions which precede exchange and result in the formation of exchange competent states, it was important to establish whether exchange occurs in the EX1 or the EX2 regime.

Mechanism of HX. The exchange regime can be established by measuring the pH dependence of the observed exchange rates, k_{obs} (see SI text). For the intact protein,¹³ the pH independence of the exchange rates of all three kinetic phases, suggested that the observed backbone amide deuteriums exchange in the EX1 limit. However, a comparison of the mean rate for each phase may obscure site-specific differences in the mechanism of exchange. In order to interpret the exchange kinetics of the individual sequence segments monitored in this study, it was, therefore, important to determine the pH dependence of k_{obs} for each sequence segment as well.

The exchange kinetics of most sequence segments appeared similar across pH 7 and pH 8 (Figure S6) and could, therefore, be fit globally to obtain the exchange rate constants. The only exception was the Met1-Glu5 segment, for which the kinetics was significantly different under the two conditions; hence, for this segment the kinetics of exchange at pH 7 and pH 8 were fit separately. For a more quantitative analysis, rate constants obtained by fitting the kinetic traces of exchange at pH 8 (Figure 2; Table 1) were compared to the rate constants determined from a global fit of the pH 7 and pH 8 kinetics (Table S2) in Figure 3. The Met1-Glu5 segment exchanged 10-fold slower at pH 7 than at pH 8, which is indicative of

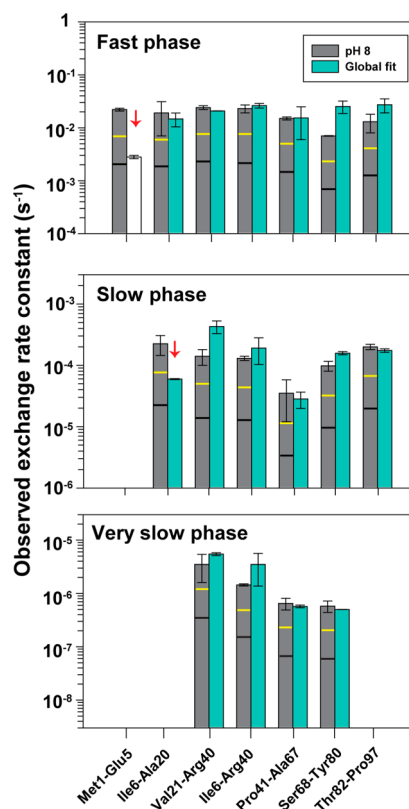


Figure 3. Comparison of exchange kinetics at pH 7 and pH 8, in 0 M GdnHCl. The exchange rate constants determined from a global fit of the kinetics of exchange measured at pH 7 and pH 8 (Figure S6) have been compared to the rate constants determined from the kinetics at pH 8 (Figure 2). For the Met1-Glu5 segment, exchange kinetics at pH 7 (white bar) and pH 8 (gray bar) were fit separately to obtain the corresponding rate constants of exchange. The error bars represent the spread in the measurements from two separate experiments. The yellow and black horizontal lines correspond to rate constants which are 3-fold and 10-fold slower, respectively, than the mean rate constant at pH 8. The red arrows indicate the segments for which significant decrease in rate is observed at pH 7, compared to pH 8.

exchange occurring in the EX2 limit. For the three deuteriums which exchanged out from the Ile6-Ala20 segment in the slow phase, the rate constant obtained from the global fit (Table S2) was 4-fold slower than that obtained from a fit of the pH 8 data alone (Table 1), as shown in Figure 3. The difference in rates for all other backbone amide sites was observed to be less than 2-fold, which appears to be within the error of the measurements.

Any change in the exchange kinetics in the transition from the EX2 to EX1 limit, i.e., in the EXX regime, as the pH is increased from pH 7 to pH 8, could be expected to manifest itself as small changes in peak shape which may not be detected by analyzing the centroids of the mass distributions alone. A comparison of the widths and heights of the mass distributions (Figures S7 and S8) ruled out any subtle changes in the mass distributions across pH 7 and pH 8. The changes in the widths of the mass distributions during the course of exchange were less than the changes expected due to random stochastic exchange,³¹ and they were the same at pH 7 and pH 8. The heights varied less than 10% around the mean height, and the heights and their variation were the same at pH 7 and pH 8. Simulations of the HX kinetics using 3-fold slower rates (see SI text) further confirmed that the majority of the observed

deuteriums in MNEI exchange in the EX1 limit at pH 8. The observed exchange rates in 0 M GdnHCl are, therefore, equivalent to the structure-opening rates of the corresponding backbone amide sites. Since the addition of denaturant further reduces k_{cl} , exchange in the presence of GdnHCl would continue to be in the EX1 regime.

Segment-Specific HX-MS Kinetics in 1 M GdnHCl.

Comparison of the structure-opening rates across 0 and 1 M GdnHCl allowed an identification of the opening events which exposed significant surface area in the protein. In the presence of 1 M GdnHCl, the following observations could be made: (1) the rates of transient opening of a subset of the observed backbone amides were affected, and (2) a subset of the observed deuteriums opened cooperatively. The kinetic traces for exchange out of the segments corresponding to $\beta 1$, α helix, $\beta 4$, and $\beta 5$ in 1 M GdnHCl are shown in Figure 4. The rate constants and relative amplitudes for each segment are reported in Table 2.

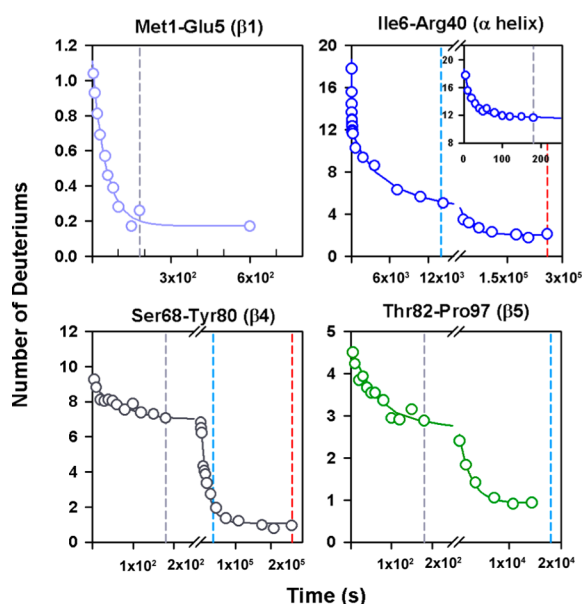


Figure 4. HX kinetics of different sequence segments of MNEI in 1 M GdnHCl, pH 8. The deuterium retention of each sequence segment was obtained with respect to time of HX in the presence of denaturant, in a way similar to that for HX in 0 M GdnHCl. The solid lines through the data represent fits to a single-, double-, or triple-exponential equation. The rate constants and amplitudes obtained from these fits are reported in Table 2. The inset shows the first 250 s of data for the Ile6-Arg40 segment. The dashed vertical lines represent different times of exchange: 3 min (gray), 8 h (blue), and 72 h (red).

The kinetics of HX during the fast and slow phases were largely unaffected by the addition of 1 M GdnHCl, except for a 25% increase in the amplitude of the slow phase, observed for the $\beta 4$ (Ser68-Tyr80) fragment (Table 2). For the very slow phase, the exchange kinetics of deuteriums in the helix (Ile6-Arg40) were 10-fold faster, while the exchange rates for the deuteriums in $\beta 4$ (Ser68-Tyr80) were 100-fold faster in the presence of denaturant. The addition of 1 M GdnHCl therefore primarily affected the very slow phase of exchange, in agreement with previous results.¹³ For the Ser68-Tyr80 segment, although six deuteriums were observed to exchange with a rate constant ($7.7 \times 10^{-5} \text{ s}^{-1}$) which is commensurate with the very slow phase (Table 2), four of these were classified

under the slow phase of exchange, in order to ensure that the total number of deuteriums which exchanged from all the fragments agreed with the number observed to exchange for the intact protein. The observation that, at the end of the slow phase (8 h), two deuteriums were left to exchange from the Ser68-Tyr80 segment (Figure 4) further supports the conclusion that these sites undergo exchange in the very slow phase.

The previous study, which monitored overall transient structure-opening rates for the whole protein,¹³ showed that while all observed deuteriums exchange one at a time in 0 M GdnHCl, 14 deuteriums exchange in an all-or-none manner in 1 M GdnHCl. The ETD ions which identified the cooperative unit have been indicated on the sequence of MNEI in Figure 5A. The Met1-Arg40 and Ser68-Pro97 ions showed unimodal distributions, while Met1-Thr82 and Asp22-Pro97 showed bimodal distributions at all time points in the presence of denaturant (Figure S10). The two forms of each ion giving rise to the bimodal distribution differed in mass by 14 Da, indicating that the entire cooperative unit observed in the intact protein was located in Pro41-Ala67 ($\beta 2$ and $\beta 3$). The rate at which the cooperative unit transiently opens to HX was determined by measuring the area under the lower mass distribution (Figure 5B) for one of the ions which displayed bimodality (Asp22-Pro97), and compared well with the rate of cooperative structure-opening observed for the whole protein.¹³

The observation of the entire cooperative unit, comprising 14 deuteriums, in a single sequence segment (Pro41-Ala67) of the protein is further strong evidence for the lack of scrambling in the present ETD study. Intramolecular migration of hydrogens and deuteriums prior to fragmentation would have precluded this observation and resulted in smaller cooperative units being observed in more than one sequence segment of the protein.

In 0 M GdnHCl, the 14 deuteriums in the Pro41-Ala67 segment were observed to exchange in three distinct phases (Table 1). Of the deuteriums in this sequence segment, 50%, which exchanged out in the very slow kinetic phase in 0 M GdnHCl, exchanged out 40-fold faster in the presence of denaturant (Table 2). On the other hand, 25% of deuteriums in this sequence segment, which exchanged out at a rate of 0.013 s^{-1} in 0 M GdnHCl, were slowed down by 3 orders of magnitude in 1 M GdnHCl. This was an unexpected observation, as the addition of denaturant should speed up and not slow down structure-opening transitions.

The kinetics of overall HX into the intact protein had indicated that the very slow phase of exchange involved the opening of 14 amide sites, which opened gradually in 0 M GdnHCl and cooperatively in the presence of denaturant.¹³ However, the kinetics of HX into the individual segments showed that the very slow phase of opening actually involves the opening of an additional seven amide sites (belonging to the helix and $\beta 4$) which could not be observed in the mass spectra of the intact protein. This could possibly be because the movement of the higher m/z peak could be monitored reliably only up to 12 h, after which the intensity of the peak reduced and it merged with the lower mass distribution, thereby precluding the detection of any further loss of deuteriums from the higher mass distribution. Since the cooperative unit was localized to only two of the ETD ions, the additional seven deuteriums were detectable in the present fragmentation data.

Denaturant Dependence of HX Rates. The kinetics of HX into the intact protein were measured over a range of denaturant concentrations, from 0 to 3 M GdnHCl, as reported

Table 2. HX Rates and Amplitudes of Different Sequence Segments of MNEI in 1 M GdnHCl, pH 8

Sequence segment	Fast phase		Slow phase		Very slow phase	
	Rate ($\times 10^{-2} \text{ s}^{-1}$)	Amplitude ^a	Rate ($\times 10^{-4} \text{ s}^{-1}$)	Amplitude ^a	Rate ($\times 10^{-5} \text{ s}^{-1}$)	Amplitude ^a
Whole protein ^b	1 ± 0.5	<i>13 ± 1</i> (33%)	1.4 ± 0.5	<i>12 ± 1</i> (31%)	3.6 ± 0.8	<i>14 ± 1</i> (36%)
Met1-Glu5 (β 1)	5 ± 2.8	<i>1</i> (100%)	-	-	-	-
Ile6-Arg40 (α helix)	4 ± 1.4	<i>6</i> (38%)	3.5 ± 0.35	<i>5</i> (31%)	2.6 ± 1.5	<i>5</i> (31%)
Pro41-Ala67 (β 2+ β 3)	-	-	-	-	2.8 ± 0.5	<i>14</i> (100%)
Ser68-Tyr80 (β 4)	1 ± 0.4	<i>2</i> (25%)	0.77 ± 0.33	<i>4</i> (50%)	7.7 ± 3.3	<i>2</i> (25%)
Thr82- Pro97 (β 5)	1.9 ± 0.14	<i>1</i> (33%)	6 ± 2.4	<i>2</i> (67%)	-	-
Mean Rate (R) ^c	2.4		1.5		2.92	

^aValues in italics correspond to the number of deuteriums which exchange; percentage of exchange is reported in parentheses. ^bValues taken from ref 13. ^cCalculated using eq 2 described in Methods.

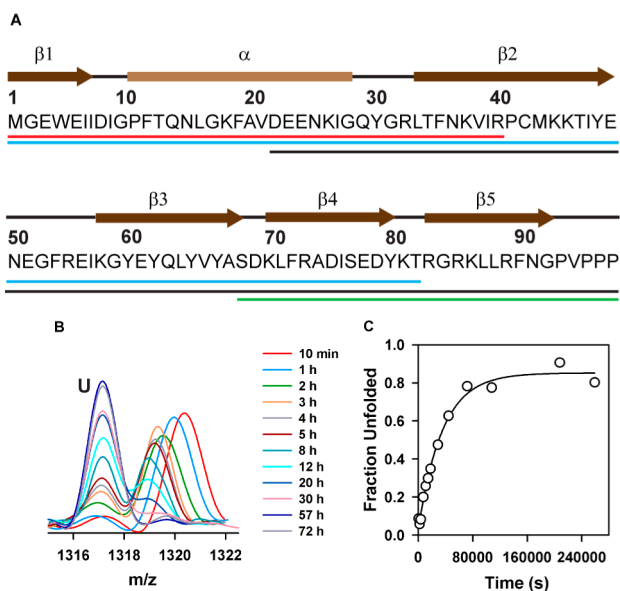


Figure 5. Exchange out from the cooperative unit in the presence of GdnHCl. (A) The peptide fragment map of MNEI is shown with the c and z ions produced by ETD denoted by colored solid lines beneath the sequence of the protein. The Met1-Arg40 (red) and Ser68-Pro97 (green) ions remain unimodal, while Met1-Thr82 (blue) and Asp22-Pro97 (black) show bimodality (Figure S10). These ions were used to identify the cooperative unit of the protein in 1 M GdnHCl, as described in the text. (B) The mass distribution for the Asp22-Pro97 ion is shown from 10 min onward for HX in 1 M GdnHCl, pH 8. (C) The increase in the fraction of the lower mass species, i.e., the unfolded state, is shown with respect to time. The solid line through the data is a fit to a single-exponential equation which yields a rate constant of $2.8 \times 10^{-5} \text{ s}^{-1}$.

previously¹³ and shown in Figure 6. While the rate constants of the fast and slow phases of exchange showed negligible

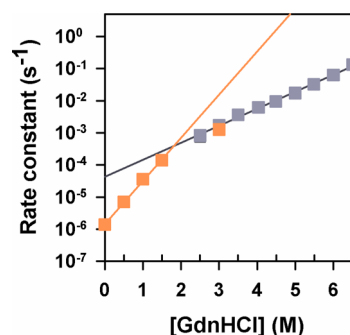


Figure 6. Denaturant dependence of HX and fluorescence-monitored rates at pH 8, 25 °C. The gray squares represent the unfolding rates of MNEI measured by fluorescence (excitation wavelength, 280 nm; emission wavelength, 340 nm) in the range of 2.5–6.5 M GdnHCl. The solid gray line corresponds to a linear regression fit of the rate constants determined by fluorescence. The orange squares correspond to the rate constants of the very slow phase of HX determined in 0–3 M GdnHCl. The solid orange line represents a linear regression fit of the very slow exchange rates in 0–1.5 M GdnHCl.

dependence on denaturant concentration (data not shown), the rate constant of the very slow phase of exchange increased steeply with an increase in denaturant concentration, up to 1.5 M GdnHCl. At all denaturant concentrations, 14 sites were observed to exchange cooperatively in the very slow phase of exchange.¹³ A comparison of the very slow HX rates with unfolding rates monitored by fluorescence further revealed that the denaturant dependence of the former was significantly larger than that of the latter. This manifested itself as a kink in the unfolding arm of the Chevron plot (Figure 6). At higher denaturant concentrations (3 M GdnHCl), the very slow

exchange rate showed good agreement with the fluorescence-measured rates.

Mapping Exchange Rates to the Protein Structure.

The kinetic traces for the individual sequence segments were used to determine the relative extent of exchange for each segment and mapped onto the protein structure for different times of HX, in 0 M (Figure 7) and 1 M GdnHCl (Figure 8).

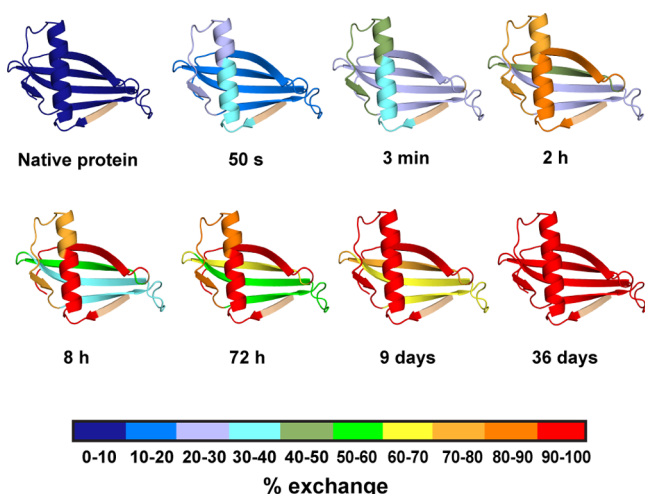


Figure 7. Sequential loss of secondary structure during transient unfolding of MNEI in 0 M GdnHCl. The percentages of exchange out from each sequence segment of fully deuterated native protein were calculated as described in the *Methods* and mapped onto the structure of MNEI in order to obtain the sequence of conformational changes which expose amide deuterium sites to exchange. The percentage of exchange is 0 for the native protein (5 s) and 100 for the unfolded state (36 days). The degree of exchange out is shown at 3 min (corresponding to the end of the fast phase), at 8 h (corresponding to the end of the slow phase), and at 36 days (corresponding to the end of the very slow phase of global unfolding) as well as at intermediate time points of exchange. HX into the helix is described by the sequence segments Ile6-Ala20 and Val21-Arg40. β 1 is shown in white to indicate that it was excluded from the analysis of opening rates since it exchanges in the EX2 limit. The color bar at the bottom indicates the increase in the percentage of exchange. The deuterium retention for each sequence segment is reported in *Table 1*.

The extent of exchange increased from 0% for the N state at 5 s of exchange, to 100% for the U state at the final time point of exchange. Mapping the exchange kinetics onto the structure of the protein (Figure 7) revealed the temporal order of structure-opening events accompanying the transient formations of I_1 (in 3 min), I_2 (in 8 h), and U (in 36 days).

The presence of 1 M GdnHCl (Figure 8) did not appear to alter the sequence of partial opening events observed in the absence of denaturant. A lack of denaturant dependence of the rates of the fast and slow phases (*Tables 1* and *2*) indicated that the transition states preceding I_1 and I_2 do not have significant surface area exposure. It was, however, interesting to note that the conformation corresponding to the higher mass species underwent further exchange from 2 to 8 h (*Figures 5B* and *8*). Hence, I_2 continues to open elsewhere even as it undergoes cooperative opening of β 2– β 3 to transiently form the globally unfolded state, suggesting that the ensemble of structures that constitute I_2 is fairly dynamic.

Comparison of HX and SX Experiments. In a previous thiol labeling (SX) study of the unfolding of MNEI,²² the dissolution of tertiary packing interactions was monitored along

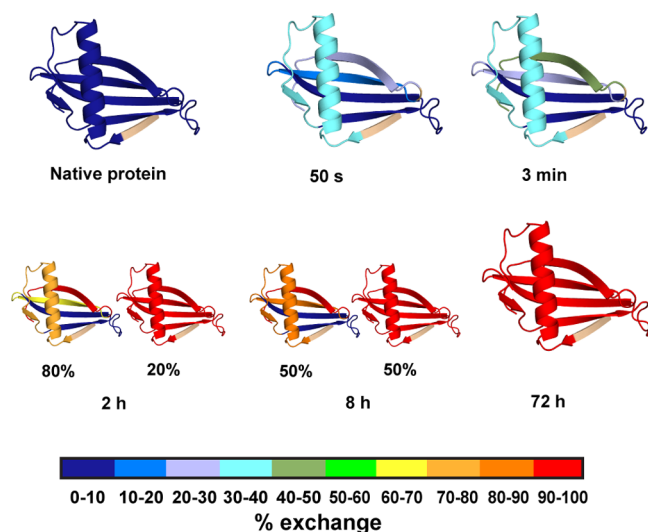


Figure 8. Sequential loss of secondary structure during transient unfolding of MNEI in 1 M GdnHCl. The percentages of exchange out from different sequence segments of fully deuterated native protein, at different times of exchange in 1 M GdnHCl, have been mapped onto the protein structure. HX into the helix is described by the sequence segment Ile6-Arg40. β 1 is shown in white to indicate that it was excluded from an analysis of opening rates since it exchanges in the EX2 limit. The structures of the two populations which differ in the exchange of the cooperative unit at 2 and 8 h of exchange are shown. The deuterium retention for each sequence segment is reported in *Table 2*.

the helix–sheet interface of the protein. The rates as well as the free energies associated with the opening of four cysteine residues (*Table S3*) were determined under native-like conditions that were identical to those of the present HX study, thus allowing a direct comparison of the current HX and previous SX data.

Figure 9 shows the extents of side-chain SX and backbone amide exchange, as a function of time, under native conditions. The transient structure-opening transitions have been defined in the context of the N state, in which there was 0% side-chain labeling and backbone amide exchange. The C13 side chain in the helix was the fastest to get labeled, within 2 s. Since the side chains in the helix, which were studied, were protected by packing against the β sheet, the opening of C13 could only have taken place by a fluctuating movement of the helix away from the sheet. The loss of packing interactions at the helix–sheet interface was, however, not accompanied by any change in the extent of HX, indicating that the intra-helical hydrogen bonding was largely intact when the helix frayed away from the β strands. Within 3 min, further side-chain packing was lost at the C42 residue, while β strands 2–5 still retained >70% of their backbone hydrogen bonding. The side chains of C74 and C63, which were the slowest to get labeled, taking 72 h to do so, also lost protection against labeling significantly faster than the backbone hydrogen-bonding network in β strands 2, 3, and 4. In fact, β 2 and β 3 had >40% of their deuteriums undergoing exchange only in the subsequent 36 days. These results indicate that tertiary packing interactions are lost faster than proximal secondary structure during transient unfolding under native conditions.

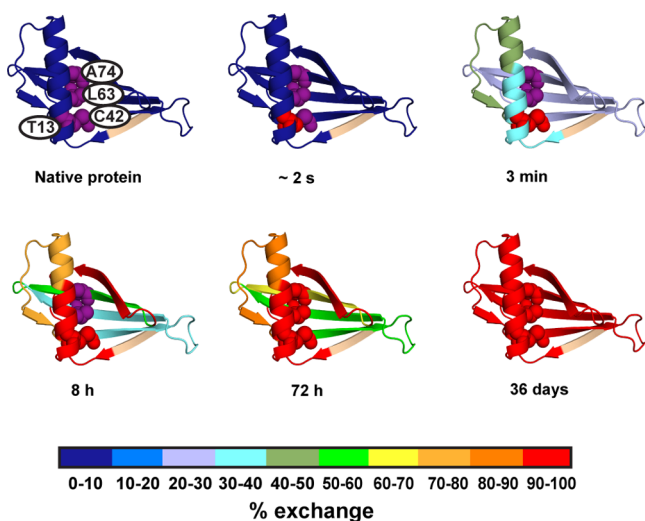


Figure 9. Comparison of HX and SX in 0 M GdnHCl, pH 8. The extents of side-chain and backbone exposure are shown at various times of labeling/exchange. The buried residue positions mutated to cysteine and probed in the thiol labeling study²² are shown as spheres in the native protein. The thiol side chain of a cysteine residue in an open (solvent-exposed) conformation is shown as a red sphere. The degree of exchange of backbone amides, from fully deuterated native protein, is indicated by the color bar shown at the bottom.

DISCUSSION

HX experiments provide valuable insight into changes in secondary structure in different parts of a protein.^{3,32–34} In previous studies, ETD was used effectively to determine the HX pattern at single amino acid resolution, by fragmenting the peptides produced after pepsin digestion.³⁵ The fragmentation of MNEI by ETD in the current work is one of the rare examples of dissociation of intact protein molecules by this method.³⁶ The structure-opening rates monitored by HX into MNEI, are widely dispersed, and a mapping of these rates on to the protein structure has allowed a determination of the hierarchy of unfolding events (Figures 7 and 8).

Identification of the Exchange Mechanism. HX experiments can determine both site-specific stabilities (in the EX2 limit^{3–6,9}) as well as the temporal order of unfolding events (in the EX1 limit^{11–13,26,37,38}). For a reliable interpretation of HX results, it is first essential to identify unambiguously the mechanism of exchange (see SI text). Mass distributions obtained in HX-MS experiments are often used to infer the exchange regime. Unimodal distributions may result from exchange in either limit, while bimodal distributions only result from exchange in the EX1 regime.^{10–13}

The bimodal mass distributions observed for the very slow phase in the presence of low concentrations of GdnHCl (Figure 5 and ref 13) are, therefore, conclusive proof of HX occurring in the EX1 limit. Hence, the k_{obs} values determined at these GdnHCl concentrations correspond to k_{op} values. The observation that the dependence on GdnHCl concentration of k_{obs} of the very slow phase extrapolates at zero denaturant to the value directly measured for k_{obs} in 0 M GdnHCl (Figure 6) provides strong evidence that exchange occurs in the EX1 regime even in the absence of denaturant, because otherwise there would not have been any agreement between the extrapolated and measured values. This was further confirmed by determining the pH dependence of the k_{obs} in 0 M GdnHCl.

pH Dependence of Exchange Rates. For the intact protein, the exchange rates of all three phases were comparable across pH 7 and pH 8.¹³ The observation that the exchange rates are comparable at pH 7 and pH 8 for each of the exchange segments, except for two segments (Figure 3 and Table S2) (see Results), for each of the kinetic phases, suggests that HX does indeed occur in the EX1 limit. It is therefore very unlikely that HX occurs by local fluctuations at rapidly fluctuating amide sites distributed all over the protein structure, because that would occur in the EX2 limit.^{3–5} Nevertheless, since the rate obtained for each kinetic phase was a mean rate measured for multiple deuteriums which exchanged in that kinetic phase, it was important to consider the possibility that a few of the amide deuteriums might exchange 10-fold slower (in the EX2 limit) or 3–5-fold slower (in the EXX limit) at pH 7. Such exchange could be obscured by the presence of multiple exchanging deuteriums in the relatively long lengths of the fragments obtained in the present study. Fortunately, the number of exchanging deuteriums in each sequence segment was split among three kinetic phases at both pH 7 and pH 8. For example, even though a total of eight deuteriums were observed to exchange from the Ser68-Tyr80 segment in 0 M GdnHCl (Table 1), only two were found to exchange in each of the fast and slow phases, at both pH 7 and pH 8. This served to effectively improve the resolution of the present study, despite the lengths of the segments observed. Moreover, if one or two deuteriums exchanged with different rates at pH 7 and pH 8 by the EX2 mechanism, even though the mean rate for a given kinetic phase of a segment of the protein would not change significantly, the number of deuteriums which exchange in that phase would reduce. Hence, a further strong indication that most observed deuteriums exchange in the EX1 limit is the observation of similar amplitudes of each kinetic phase at pH 7 and pH 8 (Table S2). The kinetic traces simulated with 3-fold slower rate constants (Figure S9, see Results) show that, while a few of the 44 deuteriums observed in the present study might exchange in the EXX regime, the bulk of the backbone amide sites exchange in the EX1 limit in 0 M GdnHCl, in an uncorrelated manner (see below).

Cooperativity of Unfolding of Individual Secondary Structural Elements. The cooperativity of transitions can be directly determined in the EX1 limit by analyzing mass distributions. A bimodal mass distribution, observed for MNEI in the presence of denaturant, is indicative of the presence of two populations of exchange competent species which interconvert via the cooperative opening of multiple amide sites. On the other hand, a unimodal distribution which shifts in mass with time, observed for MNEI in the absence of denaturant, is indicative of one or two deuteriums opening at a time in an uncorrelated manner.^{12,13} Previous studies with high-resolution structural probes had shown that, in experiments in which the entire protein structure is monitored, important features can get averaged and obscured, which are revealed only while observing individual segments or residues of the protein.³⁹ In HX-MS studies, since mass distributions analyzed for fragments of the protein correspond to lower charge states than those observed for the whole protein, the likelihood of detecting smaller cooperative units, which result in smaller separation between two peaks in a bimodal distribution, is greater. In the current study, the unimodal mass distributions of the individual ions produced by ETD, as well as the constant widths and heights of the mass distributions at all time points in the absence of denaturant (Figures S4, S5, S7, and S8), indicate

that all parts of the protein exchange gradually in 0 M GdnHCl. Hence, in the case of MNEI, the lack of overall kinetic cooperativity observed earlier for the whole protein¹³ is now seen to hold true for the individual sequence segments monitored. The unimodal mass distributions also suggest that, while the structure-opening reactions under native conditions populate multiple intermediate states, the intervening energy barriers are crossed in a gradual one-state manner, through a continuum of states.

It is interesting to note that, despite the non-cooperative nature of the structure-opening reactions under native conditions, MNEI was completely resistant to pepsin digestion in the native state. Susceptibility to proteases is generally indicative of a lack of protected structure,⁴⁰ thereby implying that a completely resistant protein should unfold in an entirely cooperative manner. It was therefore important to understand why MNEI was resistant to pepsin digestion. A simple inhibition assay (Figure S2) showed that MNEI could inhibit and therefore itself be resistant to pepsin digestion. Hence, the resistance of the native state of MNEI to pepsin digestion is not incommensurate with the non-cooperative loss of structure in the protein: MNEI binds to pepsin not as a substrate, but as an inhibitor. Indeed, MNEI belongs to the family of cystatin proteins,⁴¹ members of which are known to inhibit other acid proteases.⁴²

Nature of the Opening Reactions Which Result in Exchange. Backbone amide sites in a protein can lose protection via either local fluctuations or global structural changes.³ The faster event would dominate the exchange process, precluding the detection of the slower reaction by HX. The exchange of one or two deuteriums at a time in MNEI, in 0 M GdnHCl, suggests that the entire backbone hydrogen-bonding network in the protein could be dissolving via local openings at the backbone amide sites. A lack of denaturant dependence of the rates of the fast and slow phases of exchange is commensurate with the corresponding opening reactions causing negligible surface area exposure in the protein. However, in the case of MNEI, HX has been shown to occur in the EX1 limit at the vast majority of amide sites; hence, the local opening events which expose single amide sites at a time to exchange are structure-opening events, and are unlikely to be the same as the rapid fluctuations or breathing motions which are typically identified in the EX2 limit by the characteristically low free energy and surface exposure changes associated with them.^{3,5,43}

Indeed, several of the 44 deuteriums probed in the present study are deeply buried, making it unlikely that all of these can exchange via breathing/fluctuating motions of the protein. Moreover, the observation of three distinct opening rates indicates the presence of three different classes of backbone amide deuteriums with characteristic waiting times. The widely dispersed opening rates, k_{op} , unlike the dispersion in k_{obs} measured in the EX2 limit,^{3,5} are indicative of multiple barriers which need to be crossed in order to form the exchange competent species. Furthermore, the coupling between secondary and tertiary interactions, revealed by a comparison of SX and HX kinetics (see below), suggests that the multiple waiting times are associated with the loss of different local tertiary interactions over different time scales, and not with kinetically dispersed breathing motions. It should be noted that local changes which expose little or no surface area have also been shown to be associated with structural transitions in a protein.⁴⁴ Hence, although “local” in terms of a single site

undergoing exchange at a time, the opening events which lead to exchange in MNEI under native-like conditions are not fluctuating/breathing motions, but structural transitions which occur non-cooperatively.

The denaturant dependence of the observed HX rates of the very slow phase of exchange provides further evidence to support the conclusion that exchange in this phase is governed by global unfolding of the protein (see SI text). The formation of the globally unfolded state in 0 M GdnHCl, via uncorrelated opening of backbone amide sites, one at a time, leads to the unusual observation of uncorrelated motions resulting in a significant change in surface area, as indicated by the steep dependence of k_{op} on GdnHCl concentration. Uncorrelated opening of deeply buried residues in the protein core, which lose protection via structural unfolding, has also been observed in the case of the turkey ovomucoid third domain^{11,37} and the SH3 domain of PI3 kinase.²⁶ It was therefore concluded that, while the opening reactions in the fast and slow phases of exchange in MNEI lead to the formation of the intermediates I_1 and I_2 , the very slow phase of exchange is associated with the formation of U.¹³ This was further confirmed by simulating the experimentally observed mass distributions, for HX into MNEI in 0 and 1 M GdnHCl, according to a minimal four-state kinetic model (Figure S11), which incorporates uncorrelated opening in the EX1 limit.

Structural Heterogeneity under Native Conditions. Mapping the exchange kinetics of individual sequence segments on to the structure of the protein (Figures 7 and 8) reveals that there is no distinct structural unit in MNEI. It appears that the hydrogen-bonding network disassembles in a diffuse manner from different parts of the protein, at all stages of transient unfolding. The dispersion of the individual segment-wise rates around the mean rate for each kinetic phase (Tables 1 and 2) further indicates that the transient structural changes occur in parallel, but at slightly different rates in different regions of the protein molecule, indicating that the loss of structure occurs asynchronously across the protein structure.

The diffuse loss of secondary structure from all parts of the protein, during unfolding under native conditions, is in contrast to the foldon architecture detected in the case of several other proteins.^{3,45,46} Kinetic and equilibrium experiments have shown that for RNaseH⁴ and cytochrome c ,^{3,38,47} cooperative units of structure are lost in a hierarchical manner during unfolding to the U state. Nevertheless, a hierarchy of folding/unfolding events may not always be associated with the presence of a modular architecture in the protein, as seen here for MNEI. In the case of ubiquitin,⁴⁸ the turkey ovomucoid third domain,³⁷ and T4 lysozyme,⁴⁹ too, it has been shown that multiple amide sites with similar opening rates or protection factors are distributed all over the protein molecule, resulting in structurally heterogeneous opening transitions. For several other proteins investigated by NMR,^{50–53} residues with similar thermodynamic stabilities have been found to be structurally dispersed.

The lack of a modular folding architecture in MNEI suggests a lack of coupling between the backbone hydrogen-bonding interactions in and across different secondary structural elements, thus providing a structural basis for the non-cooperative unfolding of the protein. Amide sites within most segments open to HX in multiple kinetic phases indicating that each of these sequence segments has multiple subsets of amide hydrogen sites which open on different time scales. The observation that the unfolding of a secondary structure such as

a helix or a β strand occurs in multiple steps is noteworthy. Earlier studies had suggested this possibility in the case of a few other proteins^{54,55} and model peptides.^{56,57} The observation of diffuse non-cooperative loss of secondary structure across multiple segments, in parallel, is significant and suggests that individual secondary structures, or even parts of the same secondary structural unit, are differentially stabilized by multiple key tertiary interactions which need to break before secondary structure can dissolve.

Loss of Local Tertiary Packing Interactions Precedes Dissolution of Proximal Secondary Structure. A wide dispersion in rates is observed for the opening of backbone (Table 1) as well as side-chain (Table S3) structure. Both HX and SX²² experiments reveal the presence of multiple steps in the dissolution of secondary and tertiary interactions, respectively. Thus, while both side-chain and main-chain structures dissolve non-cooperatively in MNEI, it is also evident from Figure 9 that in all parts of the protein probed by the SX and HX experiments, the loss of local tertiary packing precedes the loss of hydrogen-bonding interactions in the vicinity. This observation suggests that the kinetic pauses observed during HX into the individual segments correspond to the waiting times for the breaking of specific tertiary packing interactions, providing a structural rationalization for the well-defined kinetic phases.

The sequential loss of tertiary and secondary interactions is also important in the context of molten globules, in which tertiary packing is significantly disrupted while secondary structure may be largely maintained.^{58–60} Previous studies have shown that both dry and wet molten globular structures are populated on the refolding^{15,21} and unfolding¹⁷ pathways of MNEI. The comparison of the HX and SX kinetics under native conditions (Figure 9) indicates that, while the intermediates I_1 and I_2 have lost tertiary packing interactions involving the side chains of C13 and C42, they retain hydrogen bonding in most secondary structural elements. These observations indicate that I_1 and I_2 have the characteristic features of a molten globular state which is partially solvated. Since HX detects structure-opening transitions which expose amide hydrogen sites to the surrounding solvent, the “dry” and “wet” regions of the molten globular intermediates are identified, thus providing a higher degree of structural resolution compared to the ensemble-averaging probes which have detected molten globules in past studies.

Structural Rationalization of Multiple Kinetic Phases. The observation of three well-defined kinetic phases for the whole protein¹³ indicated two pauses in the unfolding transition, attributed to the transient formation of two partially unfolded intermediates, I_1 and I_2 . The mechanism of transient opening of structure to HX, on consideration of overall exchange into the whole protein, was found to be describable by a sequential mechanism in which I_1 and I_2 are on-pathway to the U state (Figure S11). The well-resolved exponential kinetics of exchange had therefore suggested a stepwise transition which involves the opening of modular units of structure in the protein.

However, the uncorrelated opening of all backbone amide sites in 0 M GdnHCl was indicative of several independent opening events. The kinetic heterogeneity suggests that the intermediates I_1 and I_2 may be ensembles of structurally heterogeneous conformations. The observation of discrete steps therefore might seem inconsistent with the kinetic heterogeneity detected in the same experiment. Uncorrelated

opening alone cannot preclude the presence of a modular structure in the protein, since residues which unfold non-cooperatively may either be dispersed all over the protein structure^{37,51} or be localized to specific parts of the protein.⁶¹

In the present study, the diffuse loss of secondary structure, indicated by the uncorrelated opening of backbone amide sites in the whole protein, reveals the structural heterogeneity associated with kinetic heterogeneity. The multiple kinetic phases appear to be a result of differential stabilities of subsets of backbone amide sites in the protein. It is also evident that specific tertiary packing interactions contribute significantly to the differences in the stabilities of the subsets of the amide hydrogen sites, resulting in the observation of well-resolved kinetic phases, despite the inherent heterogeneity.

Folding in Native Conditions Will Also Be Diffuse and Asynchronous. Since the HX experiments have been carried out under native conditions, the sequence of structural events during refolding must occur in the exact reverse order of the sequence of unfolding events. The structural data obtained for unfolding in 0 M GdnHCl therefore delineates the order in which secondary structural elements are formed during refolding in 0 M GdnHCl. Moreover, the refolding reaction will also be as structurally and kinetically heterogeneous as the unfolding reaction. The current results therefore provide a structural rationale for the complex mechanisms delineated for the folding and unfolding of MNEI with ensemble-averaging probes.^{15,17,19–21} The ruggedness of the energy landscape, delineated by the one-state uphill unfolding transition¹³ would also be responsible for the slow time scales of refolding events.^{15,21}

Finally, it is interesting to note that the functional residues in MNEI, which are responsible for binding to sweet taste receptors, are dispersed across all secondary structural elements of the protein.⁶² The folding mechanisms of proteins often show a significant effect of a folding–function trade-off.⁶³ Given the absence of modular architecture and structural patterning observed in the present study, the presence of functional residues all over the protein, instead of in clusters in specific parts of the protein, is perhaps not surprising.

Smoothing of the Energy Landscape in the Presence of Denaturant. Another interesting observation made in the present study is that the structure-opening rates of a subset of backbone amides in the Pro41-Ala67 (β_2 and β_3) sequence segment, decrease upon the addition of 1 M GdnHCl (see Results). This result was unexpected as the addition of denaturant invariably increases unfolding rates. A possible explanation is that the energy landscape becomes smoothed upon the addition of denaturant (Figure 10). The presence of large barriers, which usually dominate unfolding transitions, precludes the detection of local traps which contribute to roughness of the free energy landscape. In the case of MNEI, the barriers corresponding to the fast and slow kinetic phases of opening for a part of the β_2 – β_3 segment are not observed upon the addition of denaturant, and exchange at all the amide sites in this segment becomes limited by a single barrier. The structure-opening kinetics of the β_2 – β_3 segment provides direct evidence for the decrease in the roughness of the free energy landscape upon the addition of denaturant, even in the presence of a large activation energy barrier to unfolding under native-like conditions.

Theoretical studies on protein folding show that ruggedness in the free energy landscape results in slower folding or unfolding reactions.^{64,65} In the absence of local minima which

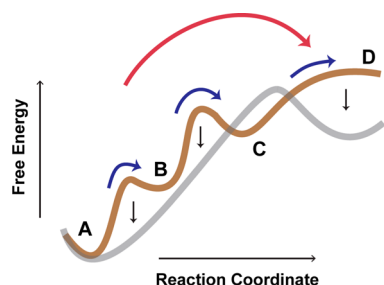


Figure 10. Smoothing of the energy landscape upon addition of denaturant. The transition from state A to state D is shown on a rough energy landscape (brown) and on a smoother landscape (gray). The blue arrows denote the conversion from A to D via intermediate states B and C on the rough landscape, while the red arrow denotes the conversion of A to D on the smoother landscape, limited by a single barrier. The structure-opening transitions observed in the Pro41-Ala67 sequence segment of MNEI occur via intermediates, on a rough landscape, in the absence of denaturant. The addition of 1 M GdnHCl appears to reduce the intervening barriers (corresponding to the black arrows in the figure), resulting in a smoother energy landscape.

contribute to the roughness, proteins would diffuse quickly over the landscape, and only the free energy barrier to folding/unfolding would determine the rate of the process.⁶⁶ Ruggedness on the free energy landscape has been experimentally observed largely in the case of downhill folding proteins which fold rapidly without any significant activation energy barrier.⁶⁵ Only in some cases has the roughness of the landscape been quantified for slow folding proteins in terms of internal friction.^{67,68} The present study provides direct evidence for the smoothing of a rough energy landscape for a protein which unfolds in an uphill manner on a very slow time scale, in the absence of denaturant.

CONCLUSION

The present study reveals the structural and kinetic heterogeneity inherent in the unfolding reaction of the protein MNEI. A wide dispersion in the structure-opening rates monitored by HX-MS has allowed a determination of the hierarchy of secondary structure dissolution in different parts of the protein. Mapping the exchange pattern onto the protein structure makes it evident that the hydrogen-bonding network dissolves in a structurally diffuse manner, precluding an unfolding mechanism based on modular loss of structure. The exchange kinetics also provides direct evidence for smoothing of a rough energy landscape upon the addition of denaturant. A subset of backbone amide sites, localized to two β strands in the protein, which open in a correlated manner upon the addition of denaturant, constitute the only cooperative unit in MNEI. The dissolution of local elements of secondary structure appears to be limited by the proximal tertiary packing interactions, resulting in the observation of well-resolved kinetic phases, despite the non-cooperative nature of the unfolding transition.

ASSOCIATED CONTENT

Supporting Information

The Supporting Information is available free of charge on the ACS Publications website at DOI: 10.1021/jacs.6b03356.

- (1) SI text, (2) SI Methods, (3) Tables S1–S3, and (4) Figures S1–S11 (PDF)

AUTHOR INFORMATION

Corresponding Author

*jayant@ncbs.res.in

Notes

The authors declare no competing financial interest.

ACKNOWLEDGMENTS

We thank Shachi Gosavi and members of our laboratory for discussions and Hemanth Giri Rao for help with MATLAB simulations. J.B.U. is a recipient of a JC Bose National Research Fellowship from the Government of India. This work was funded by the Tata Institute of Fundamental Research and by the Department of Science and Technology, Government of India.

REFERENCES

- (1) Jackson, S. E.; Fersht, A. R. *Biochemistry* **1991**, *30* (43), 10428.
- (2) Jackson, S. *Folding Des.* **1998**, *3* (4), R81.
- (3) Bai, Y.; Sosnick, T.; Mayne, L.; Englander, S. *Science* **1995**, *269* (269), 192.
- (4) Chamberlain, A. K.; Handel, T. M.; Marqusee, S. *Nat. Struct. Biol.* **1996**, *3* (9), 782.
- (5) Bhuyan, A. K.; Udgaonkar, J. B. *Proteins: Struct., Funct., Genet.* **1998**, *30* (3), 295.
- (6) Juneja, J.; Udgaonkar, J. B. *Biochemistry* **2002**, *41* (8), 2641.
- (7) Lindberg, M.; Tangrot, J.; Oliveberg, M. *Nat. Struct. Biol.* **2002**, *9* (11), 818.
- (8) Giri, R.; Morrone, A.; Travaglini-Allocatelli, C.; Jemth, P.; Brunori, M.; Gianni, S. *Proc. Natl. Acad. Sci. U. S. A.* **2012**, *109* (44), 17772.
- (9) Englander, S. W. *Annu. Rev. Biophys. Biomol. Struct.* **2000**, *29* (1), 213.
- (10) Miranker, A.; Robinson, C. V.; Radford, S. E.; Aplin, R. T.; Dobson, C. M. *Science* **1993**, *262* (5135), 896.
- (11) Arrington, C. B.; Teesch, L. M.; Robertson, A. D. *J. Mol. Biol.* **1999**, *285* (3), 1265.
- (12) Ferraro, D. M.; Lazo, N. D.; Robertson, A. D. *Biochemistry* **2004**, *43* (3), 587.
- (13) Malhotra, P.; Udgaonkar, J. B. *Biochemistry* **2015**, *54* (22), 3431.
- (14) Kimura, T.; Uzawa, T.; Ishimori, K.; Morishima, I.; Takahashi, S.; Konno, T.; Akiyama, S.; Fujisawa, T. *Proc. Natl. Acad. Sci. U. S. A.* **2005**, *102* (8), 2748.
- (15) Patra, A. K.; Udgaonkar, J. B. *Biochemistry* **2007**, *46* (42), 11727.
- (16) Kimura, T.; Maeda, A.; Nishiguchi, S.; Ishimori, K.; Morishima, I.; Konno, T.; Goto, Y.; Takahashi, S. *Proc. Natl. Acad. Sci. U. S. A.* **2008**, *105* (36), 13391.
- (17) Jha, S. K.; Udgaonkar, J. B. *Proc. Natl. Acad. Sci. U. S. A.* **2009**, *106* (30), 12289.
- (18) Jha, S. K.; Dhar, D.; Krishnamoorthy, G.; Udgaonkar, J. B. *Proc. Natl. Acad. Sci. U. S. A.* **2009**, *106* (27), 11113.
- (19) Jha, S. K.; Dasgupta, A.; Malhotra, P.; Udgaonkar, J. B. *Biochemistry* **2011**, *50* (15), 3062.
- (20) Aghera, N.; Udgaonkar, J. B. *Biochemistry* **2013**, *52* (34), 5770.
- (21) Goluguri, R. R.; Udgaonkar, J. B. *Biochemistry* **2015**, *54*, 5356.
- (22) Malhotra, P.; Udgaonkar, J. B. *Biochemistry* **2014**, *53* (22), 3608.
- (23) Bai, Y.; Milne, J. S.; Mayne, L.; Englander, S. W. *Proteins: Struct., Funct., Genet.* **1993**, *17* (1), 75.
- (24) Syka, J. E. P.; Coon, J. J.; Schroeder, M. J.; Shabanowitz, J.; Hunt, D. F. *Proc. Natl. Acad. Sci. U. S. A.* **2004**, *101* (26), 9528.
- (25) Rand, K. D.; Pringle, S. D.; Morris, M.; Engen, J. R.; Brown, J. M. *J. Am. Soc. Mass Spectrom.* **2011**, *22* (10), 1784.
- (26) Wani, A. H.; Udgaonkar, J. B. *Proc. Natl. Acad. Sci. U. S. A.* **2009**, *106* (49), 20711.
- (27) Zhang, Z.; Smith, D. L. *Protein Sci.* **1993**, *2* (4), 522.
- (28) Mayne, L.; Kan, Z.-Y.; Chetty, P. S.; Ricciuti, A.; Walters, B. T.; Englander, S. W. *J. Am. Soc. Mass Spectrom.* **2011**, *22* (11), 1898.
- (29) Hart-Smith, G. *Anal. Chim. Acta* **2014**, *808*, 44.

- (30) Abzalimov, R. R.; Kaplan, D. A.; Easterling, M. L.; Kaltashov, I. A. *J. Am. Soc. Mass Spectrom.* **2009**, *20* (8), 1514.
- (31) Weis, D. D.; Wales, T. E.; Engen, J. R.; Hotchkko, M.; Ten Eyck, L. F. *J. Am. Soc. Mass Spectrom.* **2006**, *17* (11), 1498.
- (32) Tsutsui, Y.; Dela Cruz, R.; Wintrode, P. L. *Proc. Natl. Acad. Sci. U. S. A.* **2012**, *109* (12), 4467.
- (33) Walters, B. T.; Mayne, L.; Hinshaw, J. R.; Sosnick, T. R.; Englander, S. W. *Proc. Natl. Acad. Sci. U. S. A.* **2013**, *110* (47), 18898.
- (34) Udgaonkar, J. B.; Baldwin, R. L. *Nature* **1988**, *335* (6192), 694.
- (35) Rand, K. D.; Zehl, M.; Jensen, O. N.; Jørgensen, T. J. D. *Anal. Chem.* **2009**, *81* (14), 5577.
- (36) Sterling, H. J.; Williams, E. R. *Anal. Chem.* **2010**, *82* (21), 9050.
- (37) Arrington, C. B.; Robertson, A. D. *J. Mol. Biol.* **2000**, *300* (1), 221.
- (38) Hoang, L.; Bedard, S.; Krishna, M. M. G.; Lin, Y.; Englander, S. W. *Proc. Natl. Acad. Sci. U. S. A.* **2002**, *99* (19), 12173.
- (39) Sborgi, L.; Verma, A.; Piana, S.; Lindorff-Larsen, K.; Cerminara, M.; Santiveri, C. M.; Shaw, D. E.; de Alba, E.; Muñoz, V. *J. Am. Chem. Soc.* **2015**, *137* (20), 6506.
- (40) Park, C.; Marqusee, S. *J. Mol. Biol.* **2004**, *343* (5), 1467.
- (41) Murzin, A. G. *J. Mol. Biol.* **1993**, *230* (2), 689.
- (42) Renko, M.; Požgan, U.; Majera, D.; Turk, D. *FEBS J.* **2010**, *277* (20), 4338.
- (43) Englander, S. W. *Annu. Rev. Biophys. Biomol. Struct.* **2000**, *29* (1), 213.
- (44) Maity, H.; Lim, W. K.; Rumbley, J. N.; Englander, S. W. *Protein Sci.* **2003**, *12* (1), 153.
- (45) Fuentes, E. J.; Wand, A. J. *Biochemistry* **1998**, *37* (11), 3687.
- (46) Bédard, S.; Mayne, L. C.; Peterson, R. W.; Wand, A. J.; Englander, S. W. *J. Mol. Biol.* **2008**, *376* (4), 1142.
- (47) Rumbley, J.; Hoang, L.; Mayne, L.; Englander, S. W. *Proc. Natl. Acad. Sci. U. S. A.* **2001**, *98* (1), 105.
- (48) Schanda, P.; Forge, V.; Brutscher, B. *Proc. Natl. Acad. Sci. U. S. A.* **2007**, *104* (27), 11257.
- (49) Llinas, M.; Gillespie, B.; Dahlquist, F. W.; Marqusee, S. *Nat. Struct. Biol.* **1999**, *6* (11), 1072.
- (50) Krishna Mohan, P. M.; Chakraborty, S.; Hosur, R. *J. Biomol. NMR* **2009**, *44* (1), 1.
- (51) Sadqi, M.; Fushman, D.; Muñoz, V. *Nature* **2006**, *442* (7100), 317.
- (52) Chatterjee, A.; Krishna Mohan, P. M.; Prabhu, A.; Ghosh-Roy, A.; Hosur, R. V. *Biochimie* **2007**, *89* (1), 117.
- (53) Julien, O.; Chatterjee, S.; Thiessen, A.; Graether, S. P.; Sykes, B. D. *Protein Sci.* **2009**, *18* (10), 2172.
- (54) Arrington, C. B.; Robertson, A. D. *J. Mol. Biol.* **2000**, *296* (5), 1307.
- (55) Krishna, M. M. G.; Lin, Y.; Mayne, L.; Walter Englander, S. J. *J. Mol. Biol.* **2003**, *334* (3), 501.
- (56) Thompson, P. A.; Eaton, W. A.; Hofrichter, J. *Biochemistry* **1997**, *36* (30), 9200.
- (57) Huang, C.-Y.; Klemke, J. W.; Getahun, Z.; DeGrado, W. F.; Gai, F. *J. Am. Chem. Soc.* **2001**, *123* (38), 9235.
- (58) Kuwajima, K. *Proteins: Struct., Funct., Genet.* **1989**, *6* (2), 87.
- (59) Ptitsyn, O. B.; Pain, R. H.; Semisotnov, G. V.; Zerovnik, E.; Razgulyaev, O. I. *FEBS Lett.* **1990**, *262* (1), 20.
- (60) Baldwin, R. L.; Frieden, C.; Rose, G. D. *Proteins: Struct., Funct., Genet.* **2010**, *78* (13), 2725.
- (61) Watson, E.; Matousek, W. M.; Irimies, E. L.; Alexandrescu, A. T. *Biochemistry* **2007**, *46* (33), 9484.
- (62) Spadaccini, R.; Trabucco, F.; Saviano, G.; Picone, D.; Crescenzi, O.; Tancredi, T.; Temussi, P. A. *J. Mol. Biol.* **2003**, *328* (3), 683.
- (63) Gruebele, M. C. R. *Biol.* **2005**, *328* (8), 701.
- (64) Bryngelson, J. D.; Onuchic, J. N.; Succi, N. D.; Wolynes, P. G. *Proteins: Struct., Funct., Genet.* **1995**, *21* (3), 167.
- (65) Yang, W. Y.; Gruebele, M. *Nature* **2003**, *423* (6936), 193.
- (66) Yang, W. Y.; Gruebele, M. *Biophys. J.* **2004**, *87* (1), 596.
- (67) Wensley, B. G.; Batey, S.; Bone, F. a C.; Chan, Z. M.; Tumelty, N. R.; Steward, A.; Kwa, L. G.; Borgia, A.; Clarke, J. *Nature* **2010**, *463* (7281), 685.
- (68) Chung, H. S.; Piana-Agostinetti, S.; Shaw, D. E.; Eaton, W. A. *Science* **2015**, *349* (6255), 1504.